4. SPECTRAL ANALYSIS

4.1. Introduction

The spectral analysis is widely used in the analysis of noise-like signals because it provides a frequency decomposition in harmonics the behaviour of which can be studied separately. For that reason, it has become more important than the pure statistical analysis of the surface elevation itself and therefore is quite important to find a probability distribution which depends on spectral parameters which can be predicted.

Different methods exist in order to determine the spectral density function from a discrete time record. The Fast Fourier Transform (FFT), which is an algorithm for calculating the Discrete Fourier Transform (DFT), is the most used.

4.2. Fourier theory

4.2.1. Continuous function

Joseph Fourier (1768-1830) demonstrated that almost any function can be represented as a linear combination of an infinite number of harmonic oscillations. Therefore, the surface elevation, with a zero mean level, can be written as:

$$\eta(t) = \sum_{i=1}^{\infty} a_i \cos(2\pi f_i t + \alpha_i) \tag{4.1}$$

where $\eta(t)$ is the surface elevation, f_i the frequency of the i-harmonic and α the phase.

Using trigonometric identities the last expression can be written as:

$$\eta(t) = \sum_{i=1}^{\infty} \left[A_i \cos(2\pi f_i t) + B_i \sin(2\pi f_i t) \right] \tag{4.2}$$

with $a_i = \sqrt{A_i^2 + B_i^2}$ and $\tan \alpha_i = -\frac{B_i}{A_i}$

For a record of duration D, the amplitudes A_i and B_i can be determined with the *Fourier Integrals*:

$$A_i = \frac{2}{D} \int_D \eta(t) \cos(2\pi f_i t) dt \text{ with } f_i = \frac{i}{D} \tag{4.3}$$

$$B_i = \frac{2}{D} \int_D \eta(t) \sin(2\pi f_i t) dt \text{ with } f_i = \frac{i}{D} \tag{4.4}$$

The notion of a Fourier series can also be extended to a complex function:

$$\eta(t) = \sum_{n=-\infty}^{\infty} X_n \exp\left(\frac{i2\pi n t}{D} \right) \tag{4.5}$$

where X_n denotes the complex amplitude.

4.2.2. Discrete function

In practice, the surface elevation is recorded at discrete moments in time. Then, the *Fourier Integrals* of Eq. (4.3) and (4.4) become sums:

$$X_n = \frac{1}{N}\sum_{j=0}^{N-1}\eta_j \exp\left(\frac{-i2\pi jn}{N}\right) \tag{4.6}$$

where N is the length of the discrete time series.

From Eq. (4.6) the real amplitudes a_n can be calculated as:

$$a_n = 2\sqrt{\mathrm{Re}(X_n)^2 + \mathrm{Im}(X_n)^2} \tag{4.7}$$

4.3. The wave spectrum

4.3.1. Theoretical definition

From the amplitudes a_i and phases α_i associated with a certain f_i, the amplitude and phase spectrum can be determined. In deep water, linear theory is assumed. The phase is Uniformly distributed between 0 and 2π (see Chapter 5). The amplitude is considered as a random variable too. To remove the corresponding sample character of the estimated spectrum one option would be considering $\overline{a_i}$ (from different records of surface elevation under statistically identical conditions). Instead, rather than the amplitude, the variance density is considered. The main reasons for this consideration are two. In the first place, $\frac{1}{2}\overline{a_i^2}$ is a measure of the variance (see Chapter 5) and therefore is a more representative statistical parameter of the surface elevation and it is, according to linear theory, proportional to the energy of the waves. In the second place, the variance spectrum is discrete (only the frequencies f_i are present) but, in fact, all the frequencies are present in real waves. To account for this, the variance density $\frac{1}{2}\overline{a_i^2}/\Delta f$ is defined for the interval $\Delta f = 1/D$. Finally, because of the jumps from one frequency band to the next, the following limit is taken (in which the averaged value is replaced by the expected value):

$$E(f) = \lim_{\Delta f \to 0}\frac{1}{\Delta f}E\left\{\frac{1}{2}\underline{a}^2\right\} \tag{4.8}$$

4.3.2. Practical limitations

First of all, the theoretical limit of Eq. (4.8) cannot be taken because of the finite duration of the record (taking the limit $\Delta f \to 0$ implies an infinite duration). That leads to a finite frequency resolution, removing details at a frequency scale $\Delta f = 1/D$. The frequency resolution can be improved by using a longer duration. However, the duration cannot be very long; otherwise, the record would not be stationary.

If one considers the amplitudes obtained from a single record (a_i^2 instead of $\overline{a_i^2}$), one makes an error of approximately 100% in the estimation of a spectrum (Holthuijsen, 2007) because of the estimation of the mean from a single value. Such an error is unacceptable. In fact, with the assumption of the linear theory (see Chapter 5), the estimated variance density is χ^2 distributed with 2 degrees of freedom. This is logical; the spectrum is proportional to the square amplitude, which, according to linear theory, is Rayleigh distributed.

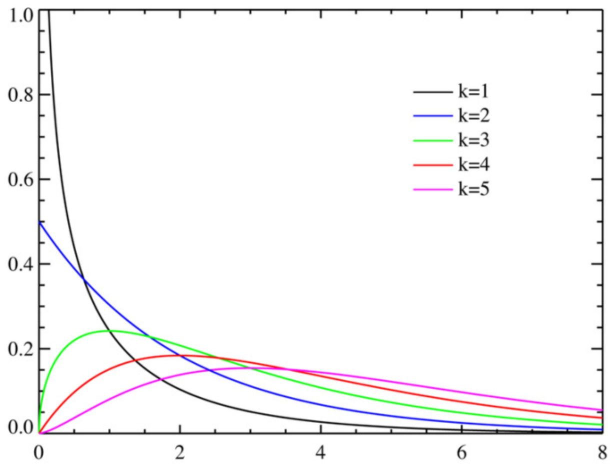

Figure 4.1 Chi-square probability density function for different degrees of freedom

A reasonable solution is dividing the initial record into p sub-records and to compute the variance density for each one. Such sub-records can be considered statistically identical and therefore one can calculate the average between their spectrums. By this manipulation the variance density spectrum is χ^2 distributed with $2p$ degrees of freedom and the error is reduced by a factor $\sqrt{p}$:

$$Error(\%) \approx \frac{100}{\sqrt{p}} \tag{4.9}$$

The price paid for the reduction of this error is the decrease of the spectrum resolution because the new frequency interval is $\delta f = p\Delta f$. In conclusion, the choice of p may be made considering both the error and the resolution. It is recommendable to have a final resolution of about 0.01 Hz (for the Mediterranean data would imply $p = 12$). However, a slightly higher factor has been considered in order to decrease the error.

Table 4.1 Parameters of the averaged spectra

Parameter	Mediterranean Sea	North Sea
p	16	16
Δf (Hz)	8.33 10^{-4}	$9.77 \cdot 10^{-4}$
δf (Hz)	0.013	0.016
Error (%)	25	25

Figure 4.2 qualitatively illustrates the influence of the variation of the parameter p. Logically, for smaller values of p, the spectrum looks more "grassy". The chosen value $p = 16$ seems quite reasonable, avoiding such fluctuations.

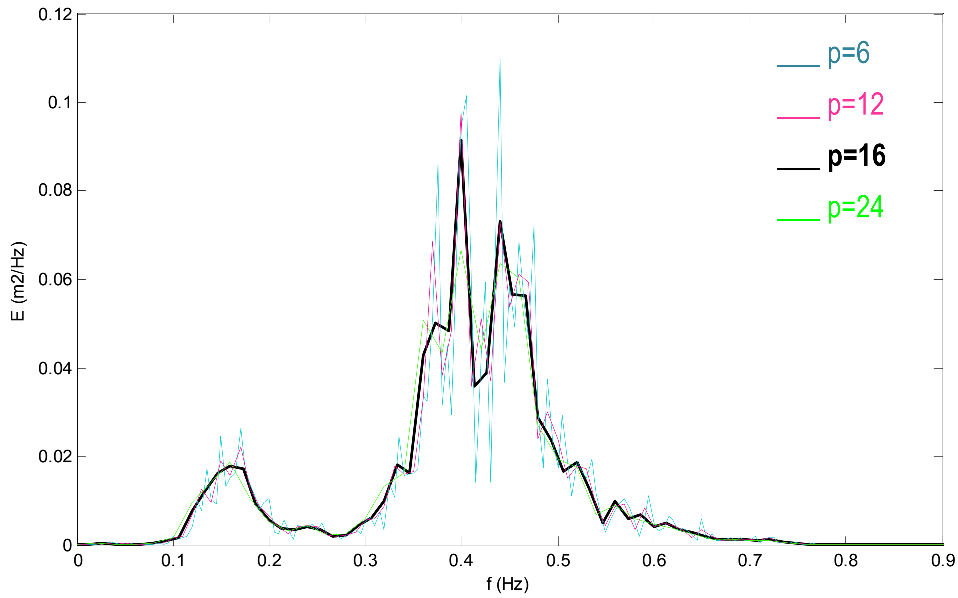

Figure 4.2 Comparison of the variance density spectrum with different values of *p*

In addition, the discrete character of the wave record introduces an error which is not so obvious. As illustrated in Section 4.2.2, the Fourier integrals are replaced by finite sums. The consequence is a phenomenon called aliasing, which consists of mirroring the energy of high frequencies around the so-called Nyquist frequency the value of which is:

$$f_N = \frac{1}{2\Delta t} \tag{4.10}$$

in which Δt is the sampling interval of the wave record. The "physical" reason is that in a discretized time record, two harmonic waves with different frequencies may pass through the same data points (see Figure 4.3). The aliasing phenomenon is caused by the inability to distinguish between them.

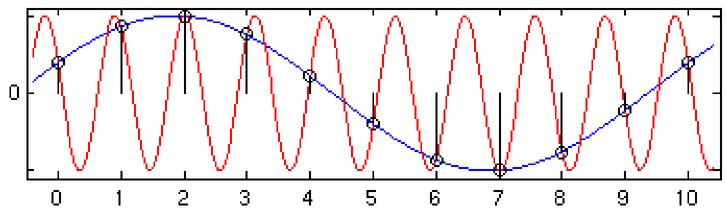

Figure 4.3 Two harmonic waves with frequencies f_1 and f_2, given at a interval time of $\Delta t = 1/(f_1 + f_2)$ are indistinguishable.

In outline, the derivation of expression of Eq. (4.10) can be explained by Figure 4.4: the discrete spectrum is not the Fourier transform of the surface elevation (understanding it as the continuous surface elevation) but the transform of the product of the surface elevation by an equally spaced delta series. The spectrum is therefore the convolution product of the true spectrum by a delta series with $1/\Delta t$ frequency interval, which leads to a mirroring effect and the superposition of energy at the frequencies near the Nyquist frequency.

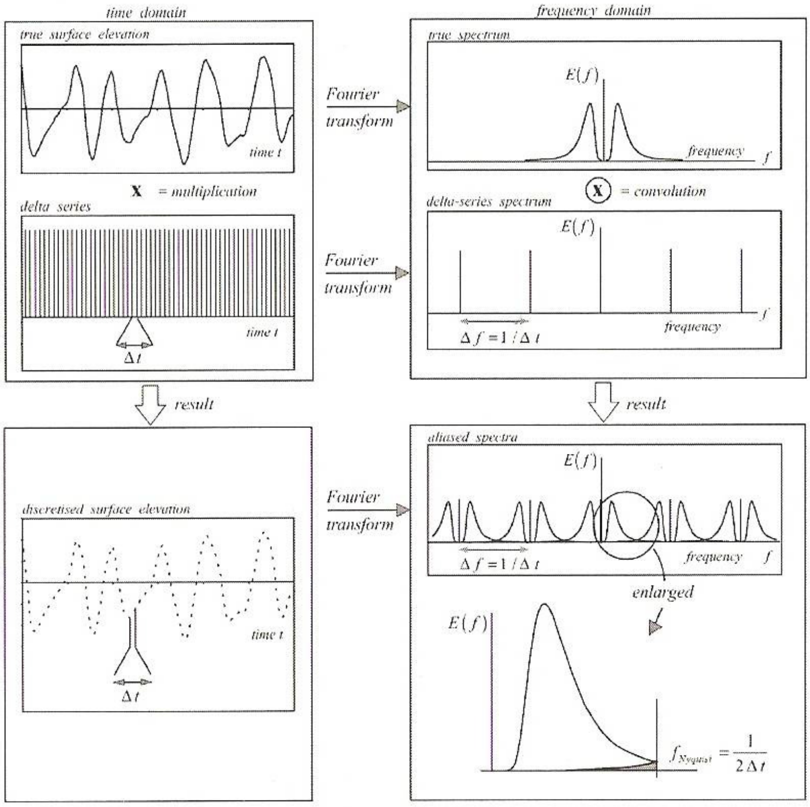

Figure 4.4 Sketch of the reason for the aliasing phenomenon (Holthuijsen, 2007)

The sampling interval of the Tortosa buoy is slightly higher than the commonly used value of 0.5 s. The reason for choosing, if possible, an interval of 0.5 s is that the Nyquist frequency becomes 1Hz. Therefore, for real sea waves, the aliasing effect on the main part of the spectrum is practically null. The problem arises when the spectrum is clearly bimodal due to the presence of sea and swell. In such a case, the energy of the higher frequencies of the storm waves may be added to the energy of the swell lower frequencies if the Nyquist frequency is similar to the one of the storm waves. In any case, the frequency domain of the calculated wave spectrum should be up-limited to the Nyquist frequency. For the analysed data the value of the Nyquist frequency is:

Table 4.2 Time interval and Nyquist frequency

Parameter	**Tortosa buoy**	**Other buoys**	**Lasers**
Δt (s)	1/1.28	1/2.56	1
f_N (Hz)	0.64	1.28	0.5

Moreover, a minimum frequency has to be considered too. The sensor of the buoy is not capable of properly measuring the surface elevation below a certain value due to changes in temperature, pressure, etc. The used lower value for the frequency is 1/D (Rotés, 2004).

4.3.3. Windowing

It has been seen that a record of length D can be mathematically described as the superposition of a number of sinusoidal waves, each having an exact number of periods in duration D ($\Delta f = 1/D$). Nevertheless, the sea actually consists of a continuous spectrum of waves. The energy of a component wavelength which does not have the exact frequency of a harmonic of D, goes to the two nearest harmonics and a portion goes to more distant ones. This leaked energy is sometimes significant and may interfere with the results. This phenomenon can be explained by considering the finite signal as the product of the entire infinite signal and a rectangular function which equals one in the duration and zero outside the duration. Therefore, the spectrum of the finite signal is the convolution product of the real spectrum and the Fourier transform of the rectangular function. In Figure 4.5, the simple case of a sinus wave is illustrated. With a duration that is a multiple of the wave length, the estimated spectrum is not affected, contrary to the case in which the duration is not a multiple of the wave length. The transform of the rectangular function appears in both cases but in the first one it does not have any affect because of those points at which the spectrum is evaluated.

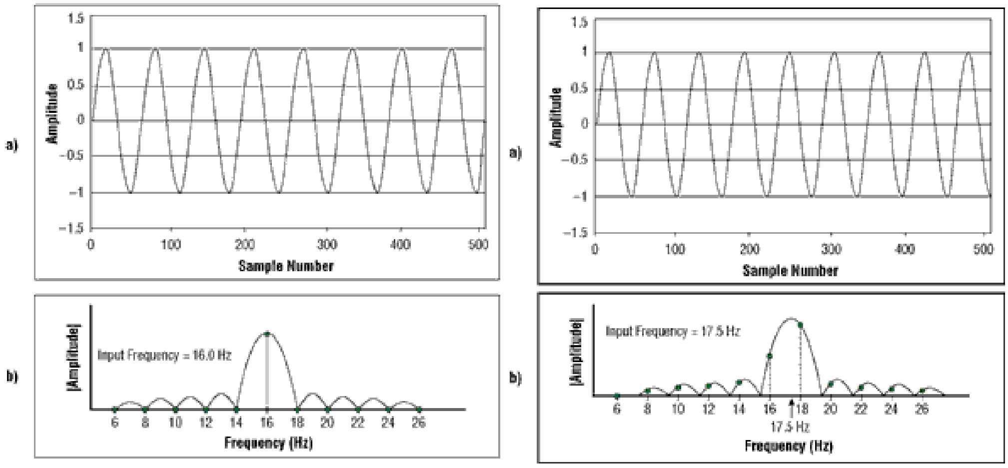

Figure 4.5 Comparison of the amplitude spectrum (logaritmic scale) between a sinus wave with a wave period a fraction of the duration (left) and any other period (right) (Lyons, 1998)

The purpose of window functions (also known as taper functions) is to reduce the above leakage of energy to other frequencies, often visible as side lobes (see Figure 4.6). They consist in multiplying the wave record by a certain function, attenuating the value of surface elevation at the ends of the record. Most of the common window functions, depending on the type of the used function, are Hamming, Hanning, Tukey (partial cosine taper), etc.

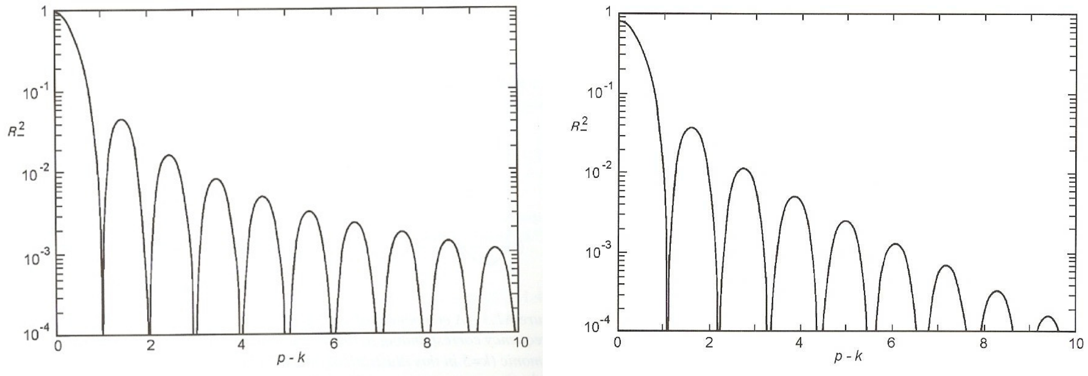

Figure 4.6 Amplitude response spectrum (logaritmic scale) of : rectangular function (left) and partial cosine taper carried out over the first and last 10% of the record (right) (Tucker & Pitt, 2001)

One of the disadvantages of window functions is that the beginning and end of the signal is attenuated. For that reason, the Tukey window has been considered in the present study because it is the one that least affects the original data. It consists of multiplying the extremes of the signal by a cosine wave. One example is illustrated in Figure 4.7.

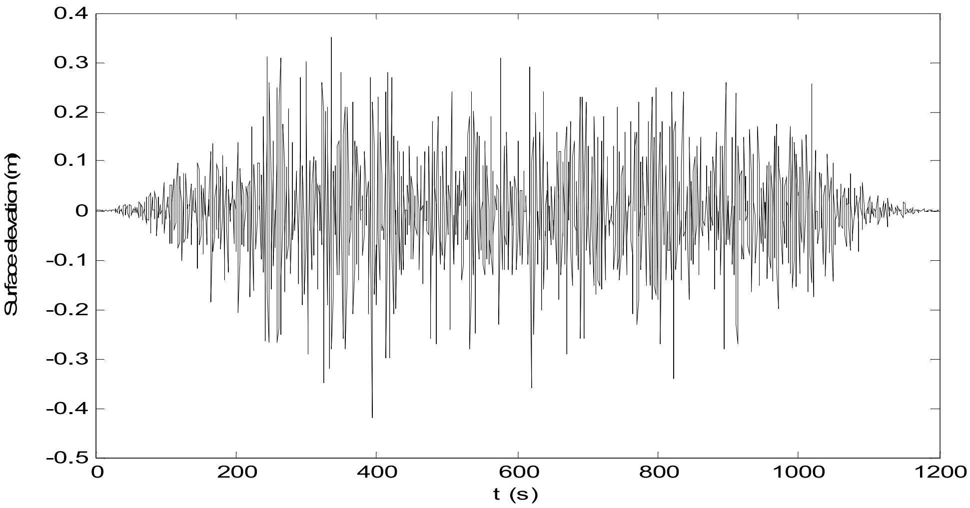

Figure 4.7 Example of a 50% cosine tapered record (25% at each end)

The total tapered length is 10%, 5% at each end. However, as one can appreciate from Figure 4.8, the spectra obtained by different percentages of tapering are practically equal.

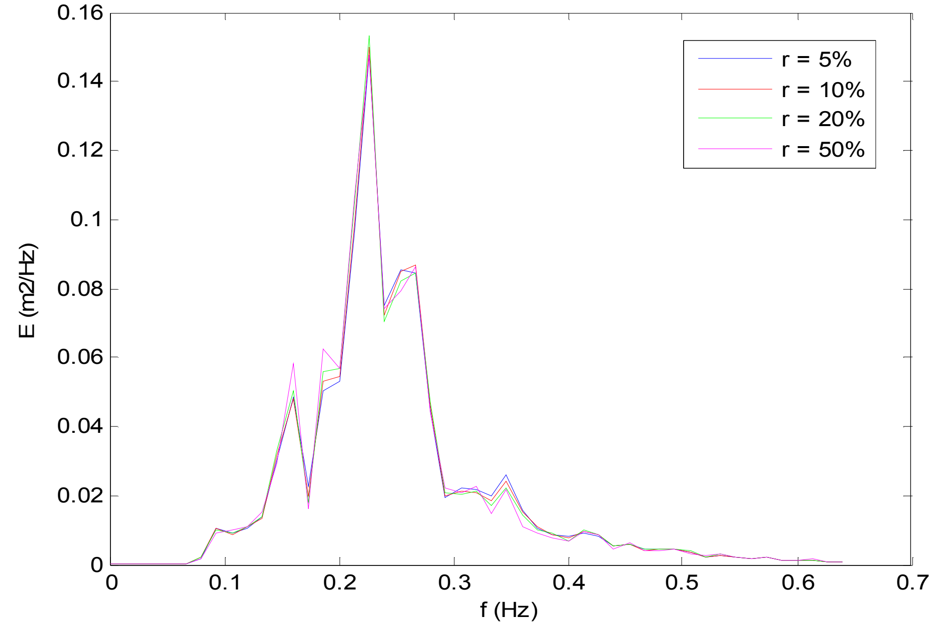

Figure 4.8 Spectrum of a partial cosine tapered record with different percentages of tapering.

The used function $f(k)$ in the Tukey window (implemented in MATLAB) is:

$$f(k)=\begin{cases}\frac{1}{2}\left[1+\cos\left(\frac{2\pi}{r}\frac{(k-1)}{(N-1)}-\pi\right)\right] & k<\frac{r}{2}(N-1)+1\\ 1 & \frac{r}{2}(N-1)+1\leq k\leq N-\frac{r}{2}(N-1)\,,\\ \frac{1}{2}\left[1+\cos\left(\frac{2\pi}{r}-\frac{2\pi}{r}\frac{(k-1)}{(N-1)}-\pi\right)\right] & k>N-\frac{r}{2}(N-1)\end{cases} \tag{4.11}$$

for $k=1...N$

in which k is the index for each data point, r is the proportion of tapering (0.1, 0.05 at each end), and N the record length. The window multiplies the variance of the record by a factor:

$$G=1-5r/8 \tag{4.12}$$

Therefore, the final spectrum has to be divided by the above mentioned factor of Eq. (4.12).

In Figure 4.9, the effects of both aliasing (due to discretisation of a signal) and leakage (due to truncation) are illustrated.

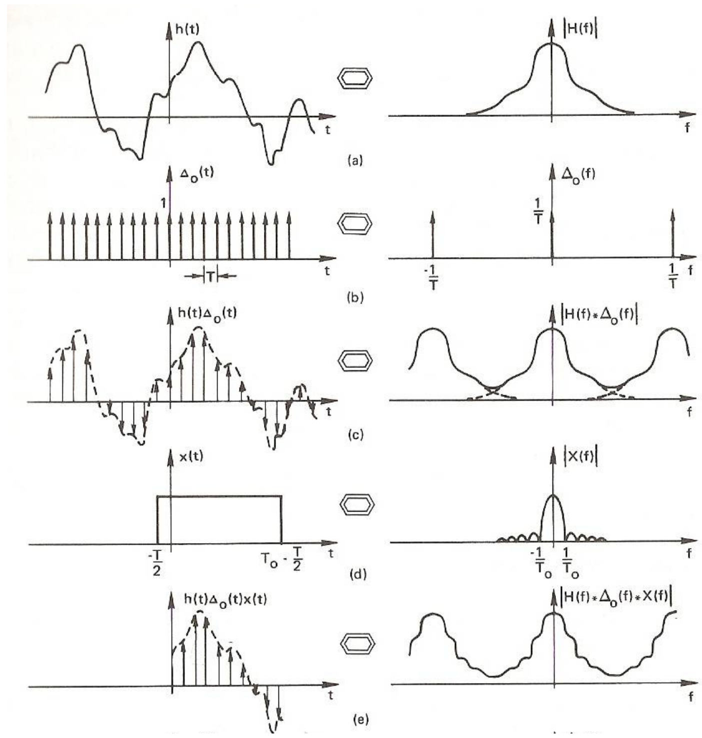

Figure 4.9 Aliasing (due to discrete record) and leakage (due to finite duration) (Brigham, 1988)

4.4. Wave spectrum calculation

In the present study, the FFT algorithm of MATLAB has been used, which implements the Fourier Transform of Eq. (4.6) (multiplied by a scale factor N). The summation differs slightly from Eq. (4.6) because the numeration begins with 1.

$$X_n = \sum_{j=1}^{N} \eta_j \exp\left(\frac{-i2\pi(j-1)(n-1)}{N} \right) \tag{4.13}$$

As previously said, the analysis is organized by year-buoy. Each one is organized into a matrix with dimensions: length of the record x number of records. For example, in the Mediterranean data, the number of the analysed matrix totals 27 (number of year-buoys). The FFT is computed for each matrix, in which the Fourier Transform is calculated for each column.

The calculation of Eq. (4.13) for all n-frequencies can be interpreted as the product of a matrix (the exponential part) multiplied by vector (the surface elevation).The efficiency of the FFT lies in the proper decomposition of such a matrix and other relevant permutations that considerably reduce the number of operations needed (for more detail information consult Birgham, 1988). The possible decompositions depend on the length of the vector. Therefore, the execution time and the required memory for the FFT (directly related to the required number of operations) depend on the length (in terms of number of data points) of η. The FFT is fastest for records in which the number of data points is a power of two and almost as fast for lengths that have only small prime factors. As the prime factors are smaller, the matrix can be further decomposed and a fewer number of operations are required.

This aspect may not seem relevant but it is. As the amount of data to be analysed increases, one has to consider these limitations. In fact, without taking into account the considerations explained below, in some “years-buoy” the FFT could not be computed in one step due to memory problems.

MATLAB offers the option of using a function called FFTW which optimises the FFT. This optimization is related to the chosen decomposition of the original length. Bear in mind that for the same length, the required number of operations varies, depending on the factorization used. For example, in a simple case of a length of 16, the base-4 algorithm requires approximately 30 % fewer multiplications than the base-2 algorithm (Brigham, 1988). The original lengths of the records are:

Table 4.3 Original length of the records

Parameter	Tortosa (1991-2000)	Tortosa (2001-2006)	Other buoys	Lasers
Length	1536	1535	3072	1024

Except in the case of Tortosa (2001-2006), the prime factors involved are small: 1536 (=$2^9 \cdot 3$), 3072 (=$2^{10} \cdot 3$) and 1024 (=2^{10}). However, the length of 1535 ($5 \cdot 307$) cannot be decomposed into small prime numbers. For these records the zero padding technique is used. It consists of adding zeros until the desired length is achieved. In this case, only one zero is added in order to have a length of 1536. The only effect is the scaling of the results of Eq. (4.6). However, as the FFT implemented in MATLAB does not include the factor N (see Eq. (4.13)), the results are not scaled. The spectrum therefore is obtained by considering the original length and the original frequency interval for the amplitude calculation and no scaling factor is required.

Remark that by adding zeros the resolution is not increased (although the frequency band becomes smaller). Essentially, this is an interpolation procedure (Shiavi, 1991) (see Figure 4.10).

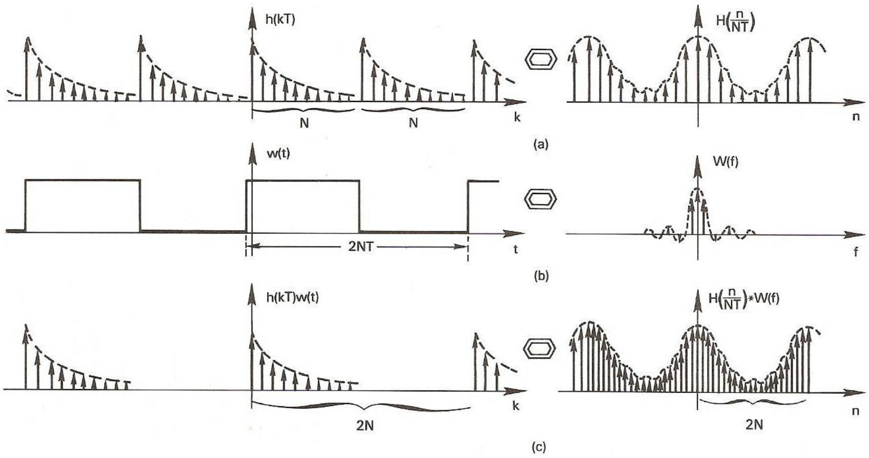

Figure 4.10 Example illustrating the false resolution enhancement by adding zeros (Brigham, 1988)

From the complex amplitude X_n provided by the FFT, the real part is considered because it is directly related to the amplitude associated to each frequency (see Eq. (4.7)). In addition, only the amplitudes associated with the interval frequency $1/D < f < f_N$ are considered (as explained in Section 4.3.2). The wave spectrum is calculated as:

$$E(f_i) = \frac{1}{\Delta f}\frac{1}{2}a_i^{\,2} \tag{4.14}$$

However, this is not the final result. The final spectrum is found by averaging the amplitudes' values in the interval band $\delta f = p\Delta f$. This is mathematically the same operation as dividing the records in subrecords, computing the wave spectrum for each subrecord and taking the average (see Section 4.3.2). Figure 4.11 illustrates the difference between the initial and the final (i.e. averaged) wave spectrum.

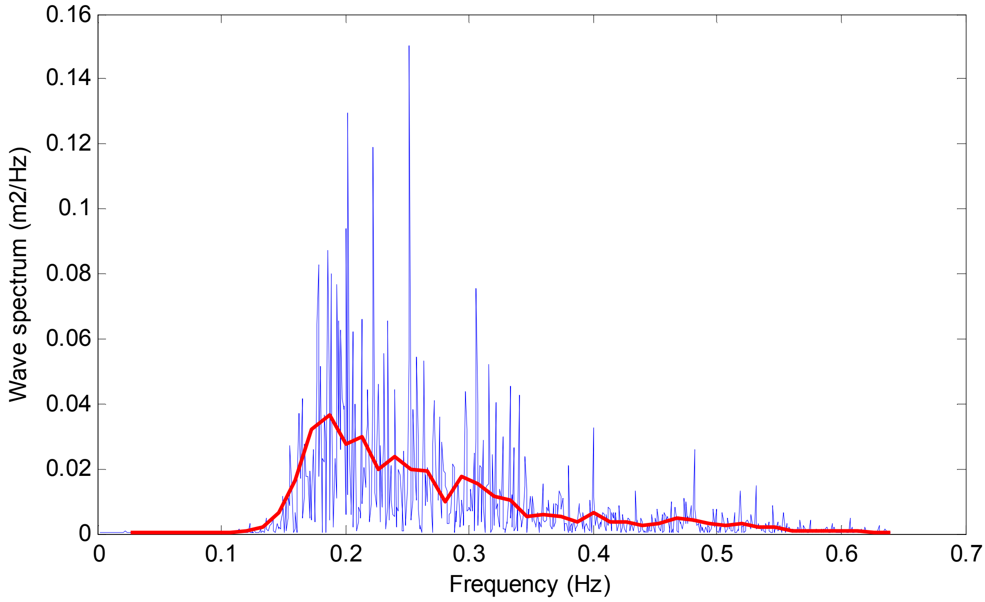

Figure 4.11 Averaged spectrum (red) compared to the initial one (blue) (Tortosa: 21/09/1991 00:16 h)

4.5. Spectral parameters

The spectral parameters can be split in two groups, depending on whether they characterize the surface elevation (H_{m_0}, T_m, T_0, T_c) or the spectral shape (ε, ν, Q_p). In addition, the BFI is computed, which is related to the occurrence of extreme waves such as, freak waves for example.

In most of parameter calculations, spectral moments are used. They are defined as:

$$m_n = \int_0^\infty f^n E(f)df \quad \text{for} \quad n = \ldots,-3,-2,-1,0,1,2,3,\ldots \tag{4.15}$$

One of the most used is the zeroth-order moment, which is the variance of the surface elevation (see Chapter 5).

4.5.1. Parameters related with the surface elevation

First of all, note that the expressions shown bellow of the most important parameters are derived assuming linear theory.

- Mean wave height

$$H_{mean} = \sqrt{2\pi m_0} \tag{4.16}$$

- Significant wave height

$$H_s \approx 4\sqrt{m_0} \tag{4.17}$$

- Root-mean-square wave height

$$H_{rms} = \sqrt{8m_0} \tag{4.18}$$

- Expected maximum wave height:

$$E\{H_{\max}\} = 2\left(1 + \frac{0.29}{\ln N}\right)\sqrt{2\ln N}\sqrt{m_0} \tag{4.19}$$

- Mean zero-crossing period

$$T_0 = \sqrt{\frac{m_0}{m_2}} \tag{4.20}$$

- Mean wave period (inverse of the mean frequency), which is less dependent on high-frequency noise than the previous one.

$$T_m = \frac{m_0}{m_1} \tag{4.21}$$

- Significant wave period

$$\begin{aligned} T_s &= T_{peak} \quad \text{for swell} \\ T_s &= 0.95T_{peak} \quad \text{for wind sea} \end{aligned} \tag{4.22}$$

where T_{peak} is the inverse of f_{peak}

4.5.2. Shape parameters

- Goda's parameter (Goda, 1970):

$$Q_p = \frac{2}{m_0^{\ 2}} \int_0^\infty E^2(f) f df \tag{4.23}$$

- Longuet-Higgins's spectral width (1975):

$$\nu = \sqrt{\frac{m_0 m_2}{m_1^2} - 1} \tag{4.24}$$

- Cartwright and Longuet-Higgins (1956) defined another spectral width parameter:

$$\varepsilon = \sqrt{1 - \frac{m_2^2}{m_0 m_4}} \tag{4.25}$$

which is used in the probability density function of the wave crest defined as local maxima. In general, ν is preferable above ε because it depends on lower order moments and therefore less on the tail of the spectrum.

4.5.3. BFI

For a more detailed explanation of this parameter see Chapter 6. The calculation of BFI is made according to the following expression (Goda, 1970; Janssen, 2003, 2005):

$$BFI = Q_p k_{m_{01}} \sqrt{2\pi m_0} \tag{4.26}$$

where Q_p is the peakedness parameter of Goda (Eq. (4.23)), $k_{m_{01}}$ the mean wave number:

$$k_{m_{01}} = \frac{(2\pi)^2}{g{T_0}^2} \tag{4.27}$$

and T_0 the mean zero crossing period.